IJPSR (2016), Vol. 7, Issue 8 **(Research Article)**

INTERNATIONAL JOURNAL OF PHARMACEUTICAL SCIENCES AND RESEARCH

Received on 07 March, 2016; received in revised form, 30 May, 2016; accepted, 08 July, 2016; published 01 August, 2016

IN-SILICO PHARMACOPHORE MAPPING AND DOCKING STUDIES OF INDOLE/BENZOXIMIDAZOLE-5-CARBOXIMIDINE DERIVATIVES AS ANTI-CANCER AGENTS

Shivangi Agarwal[1], Mitali Mishra[1], Vikash K. Mishra [1], D. Vinod [2], Ekta Verma [1] and Sushil K. Kashaw [*1]

Department of Pharmaceutical Sciences [1], Dr. H.S. Gour Central University, Sagar, Madhya Pradesh, India

Madras Medical College [2], Chennai, Tamil Nadu, India

Keywords:

Pharmacophore Mapping, Docking, Indole/benzoximidazole-5-carboximidine, Anti-cancer, Glide scores and Urokinase type plasminogen activator (uPA)

Correspondence to Author:
Dr. Sushil K. Kashaw

Assistant Professor,
Department of Pharmaceutical Sciences, Dr. H.S. Gour Central University, Sagar, Madhya Pradesh, India.

Email: sushilkashaw@gmail.com

ABSTRACT: The present research has been focused on the development of pharmacophore mapping and docking studies of indole/benzoximidazole-5-carboximidine derivatives as anti-cancer agents that can explore basic pharmacophore responsible for biological activity of structurally diverse compounds and also their binding affinity to the urokinase-type plasminogen activator (uPA). For pharmacophore mapping, a highly predictive pharmacophore based 3D-QSAR model was generated. Molecular docking experiments were carried out by means of the Glide module of the Schrodinger. A cubing receptor grid was centred around the co-crystallized ligand where the active binding site is present. The XP (extra precision) scoring function of GLIDE 6.0 was used. The scoring function of GLIDE docking program is presented in the G-score form which indicates the binding affinity of the designed compound to the receptor. A five point pharmacophore (APRRR) with one acceptor atom, one positively charged group and three aromatic rings as pharmacophore was developed. The generated best pharmacophore hypothesis yielded a statistically significant QSAR model, with a correlation coefficient of R2 = 0.8548 for training set molecules. The same sets of molecules were docked with urokinase-type plasminogen activator as target protein. The Gscore of the ligand 25 was found to be -11.89 as comparable with the G-score of reference drug (132: 6-CHLORO-2 -(2-HYDROXY-BIPHENYL -3-YL) -1H-INDOLE-5-CARBOXAMIDINE) i.e.-11.626. The present study aimed to develop ligand based pharmacophore hypothesis and an interaction pattern by docking. Both studies rendered significant information which highlights important binding features of uPA inhibitors which can be utilized further in the successful designing of novel highly active analogues against uPA.

INTRODUCTION: The involvement of urokinase-type plasminogen activator receptor in the pathology of human cancers is well documented [1, 2, 3].

QUICK RESPONSE CODE

DOI: 10.13040/IJPSR.0975-8232.7(8).3243-61

Article can be accessed online on: www.ijpsr.com

DOI link: http://dx.doi.org/10.13040/IJPSR.0975-8232.7 (8).3243-61

High levels of uPAR in tumour tissues and plasma from patients with various human cancers are associated with poor prognosis and increased risk of tumour recurrence and metastasis.

The uPAS (urokinase plasminogen activating system) is involved in the extracellular conversion of the ubiquitous inactive plasminogen to the broad-spectrum serine protease plasmin, implicated in numerous pathophysiological process requiring the remodelling of extracellular matrix (ECM) and basement membranes (BM) [4].

Human uPAR (urokinase-type plasminogen activating receptor) is a glycolipid-anchored modular protein having a single-chain polypeptide (283 amino acids) organized into three extracellular domains [5]. These three domains form a concave shape with a central cone-shaped cavity where the urokinase fragment inserts [6]. Inhibition of expression of these components leads to a reduction in the invasive and metastatic capacity of many tumors [7]. The causes of cancer are diverse, complex and only partially understood. Risk to cancer can be increase by tobacco use, dietary factors, certain infections, exposure to radiations, environmental factors, obesity etc [8].

These factors can either directly damage the genes or combine with genetic faults within the cells to cause cancerous mutations [9]. Only about 5% to 10% of all cancers are inherited – resulting directly from gene defects (called mutations) inherited from a parent [10]. Cancer is the second leading cause of death in the developed world. Cancer accounted 7.9 million deaths (around 13% of all deaths) in 2008 [11]. Regular use of some established screening tests can prevent the development of cancer through identification and removal or treatment of premalignant abnormalities [12]. Currently in spite of intensive research and some major advances in treatment, cancer claims the life of nearly one out of four Americans.

It is thus second to heart diseases responsible for 35% of deaths in US [13]. These numbers are projected to rise to 15 million new cases and 9.0 million deaths in 2015 and 21.4 million new cases and 13.1 million deaths in 2030, respectively. Increased consumption of coffee may reduce the risk of liver cancer [14]. Urokinase-type plasminogen activator (uPA), a trypsin-like serine protease is strongly associated with tumor cells plays a vital role in several biological processes including tissue remodeling, cell migration, and matrix degradation[15]. Over expression of uPA (urokinase-type plasminogen activator) or uPAR (urokinase-type plasminogen activator receptor) is a feature of malignancy and is correlated with tumour progression and metastasis [7]. Because of its involvement, uPA (urokinase-type plasminogen activator) has emerged as a drug target for development of therapeutics for various types of cancer. This has resulted in an immense clinical interest in developing potent and orally bioavailable inhibitors of uPA (urokinase-type plasminogen activator) that can serve as therapeutic agents in the treatment of cancer [15]. Quantitative structure-activity relationships (QSARs) are based on the assumption that the structure of a molecule (i.e. geometric, steric and electronic properties) must contain the features responsible for its physical, chemical and biological properties and on the ability to represent the chemical by one or more numerical descriptors [16].

It also borders into various other areas of chemoinformatics and bioinformatics [17]. Pharmacophore approaches have become one of the major tools in drug discovery after the past century's development. The concept of pharmacophore was first introduced in 1909 by Ehrlich who defined the pharmacophore as 'a molecular framework that carries (phoros) the essential features responsible for a drug's (pharmacon) biological activity'. A Pharmacophore model can be established either in a ligand manner, by superposing a set of active molecules and extracting common chemical features that are essential for their bioactivity, or in a structure-based manner, by probing possible interaction points between the macromolecular target and ligands. Pharmacophore approaches have been used extensively in virtual screening, de novo design and other applications such as lead optimization and multitarget drug design [18].

Pharmacophore modeling is one of the most powerful techniques to classify and identify key features from a group of molecules such as active and inactive compounds [19]. Phase is a versatile product for pharmacophore perception, structure alignment, activity prediction, and 3D database searching [20]. In the field of molecular modeling, docking is a method which predicts the preferred orientation of one molecule to a second when bound to each other to form a stable complex[21]. Docking is frequently used to predict the binding orientation of small molecule drug candidates to their protein targets in order to in turn predict the affinity and activity of the small molecule. Hence docking plays an important role in the rational design of drugs [22].

The aim of molecular docking is to achieve an optimized conformation for both the protein and ligand and relative orientation between protein and ligand such that the free energy of the overall system is minimized [23, 24]. To perform a docking screen, the first requirement is a structure of the protein of interest. Usually the structure has been determined using a biophysical technique such as x-ray crystallography, or NMR spectroscopy. This protein structure and a database of potential ligands serve as inputs to a docking program [23].

In the present study, we have carried out pharmacophore mapping [25, 26] and docking studies[27] employing PHASE and GLIDE modules of Schrödinger's software program 'MAESTRO' respectively in order to explore the correlation between structure and biological activity of indole/benzoimidazole-5-carboxamidines as uPA (urokinase-type plasminogen activator) inhibitors and the docking studies were carried out to explore the binding interaction mechanism between analogues and the receptor. The final evaluation is done with glide score (docking score) and best pose is generated as the output. We have developed 3D-QSAR models for the series of indole/ benzoimidazole-5-carboxamidines and the contour maps derived revealed the significance of hydrogen bond donor, hydrophobic/non-polar (B) and electron withdrawing (C) properties. The blue contours represent the regions where the substitution of groups with the particular property may enhance the biological activity whereas red cubes represent the depreciating biological activity. The 3D-QSAR models generated in the present study are consistent with the binding site and can be used as putative pharmacophore. The structural requirements identified in the present study can be utilized strategically in the design of novel, potent, and selective urokinase plasminogen activator inhibitors as anticancer agents.

MATERIALS AND METHODS:

Selection of molecules and data set:

A dataset of thirty nine indole/benzoximidazole-5-carboximidine derivatives [15] reported to have inhibitory activity on urokinase plasminogen activator (uPA) was used in the present Pharmacophore Mapping and Docking Studies. The inhibitory concentration values reported [15] as $_{P}IC_{50}$ ($-\log IC_{50}$) were used for the studies. The structures along with their $_{P}IC_{50}$ values are represented in **Table 1**.

TABLE 1: CHEMICAL STRUCTURES OF DATA SET USED FOR PHARMACOPHORE MAPPING AND DOCKING STUDIES WITH ACTUAL AND PREDICTED ACTIVITY FROM THE BEST MODEL

Molecule	Structures	Activity(pIC50)	
		Actual	Predicted
S1	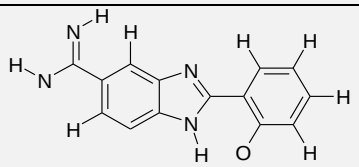	-0.74	-0.81
S2	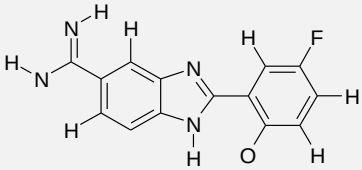	-0.447	-0.55
S3	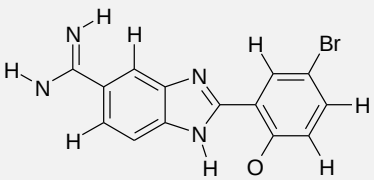	-0.568	-0.64
S4	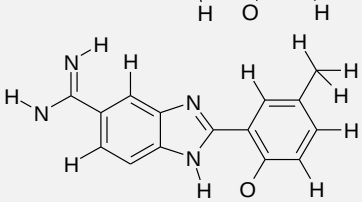	-0.87	-0.44

S5	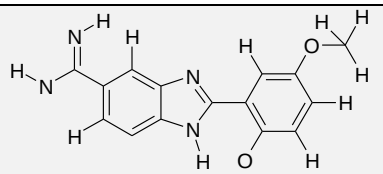	0.556	0.89
S6	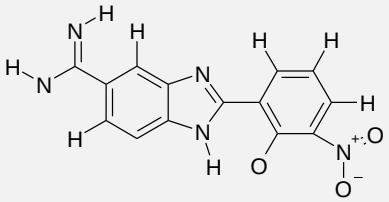	0.045	-0.32
S7	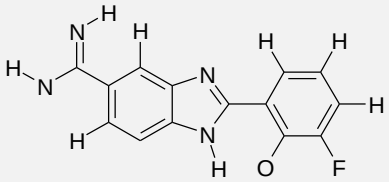	0.259	-0.09
S8	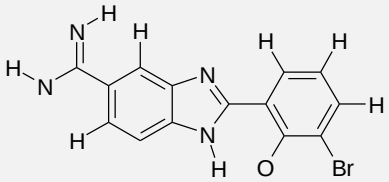	0.25	0.36
S9	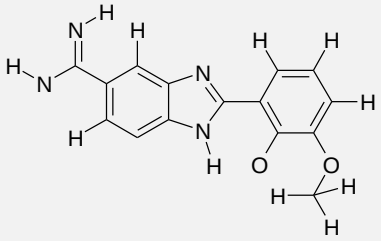	-0.556	0.02
S10	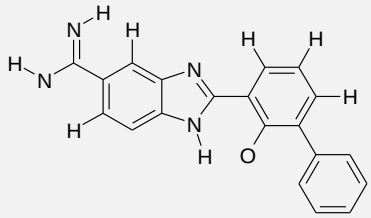	0.39	0.92
S11	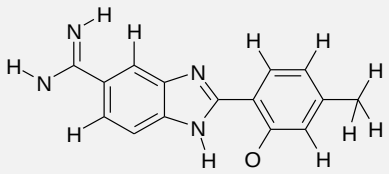	-0.556	-0.80
S12	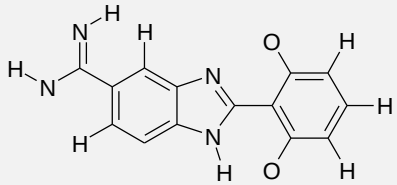	-0.278	-0.05
S13	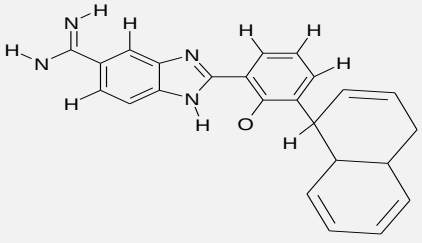	-0.591	-0.48

S14	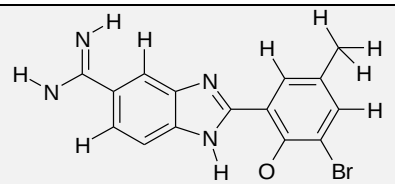	0.552	0.52
S15	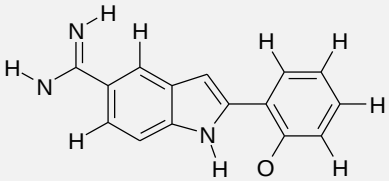	-0.38	-0.31
S16	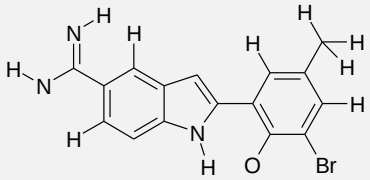	1.25	0.79
S17	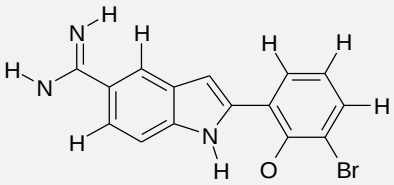	1.45	0.51
S18	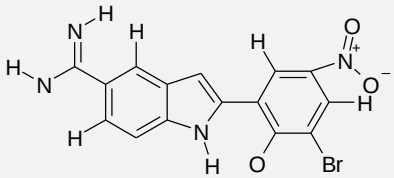	0.552	0.84
S19	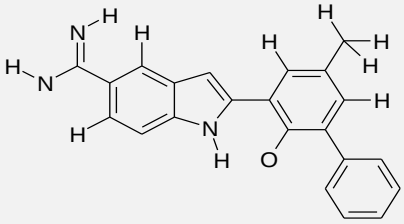	1.42	1.70
S20	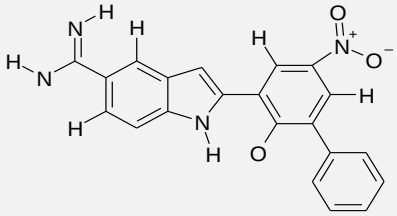	1.602	1.73
S21	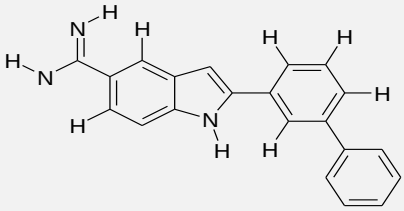	-1.113	-1.02
S22	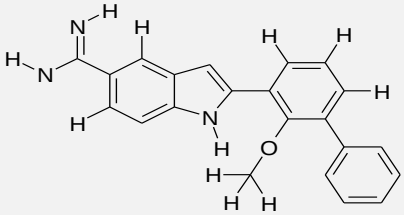	-0.5	-0.82

S23	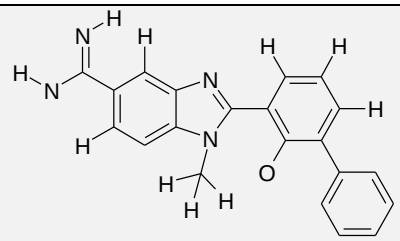	-1.041	-0.80
S24	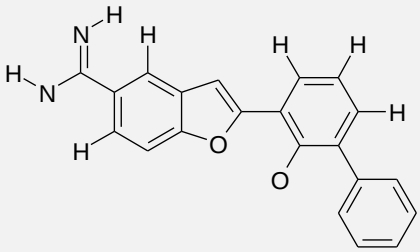	0.259	0.25
S25	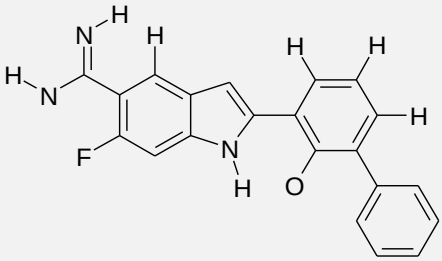	1.698	1.75
S26	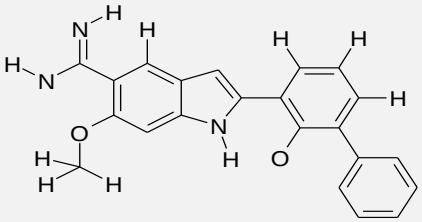	0.44	0.24
S27	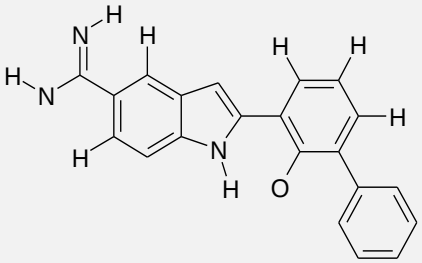	2.096	1.29
S28	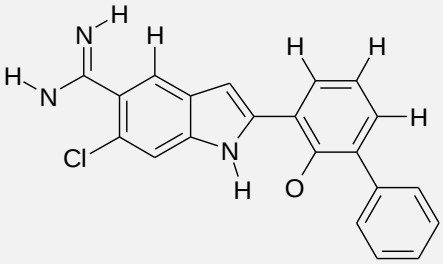	2.045	1.98
S29	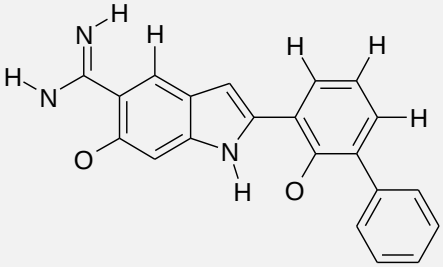	-0.3	-0.21

S30	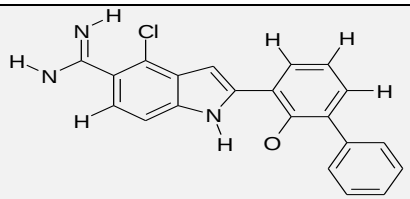	-0.477	0.70
S31	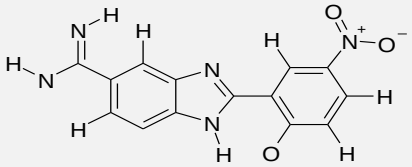	-0.518	-0.48
S32	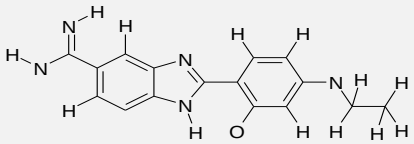	-1.13	-1.25
S33	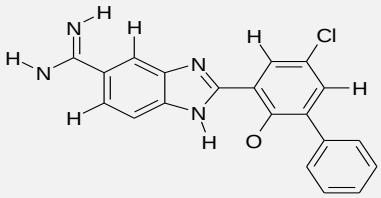	0.301	0.61
S34	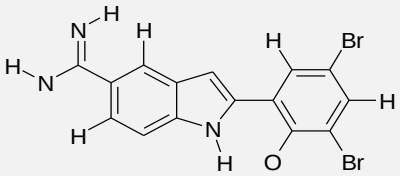	1	0.84
S35	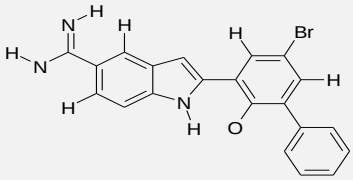	1.36	1.59
S36	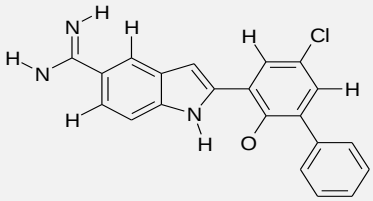	1.25	1.54
S37	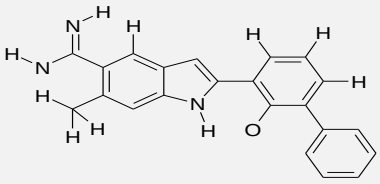	1	1.09
S38	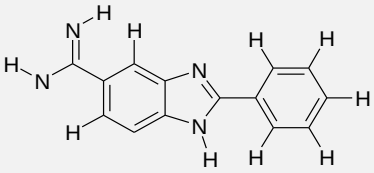	-0.903	-1.06
S39	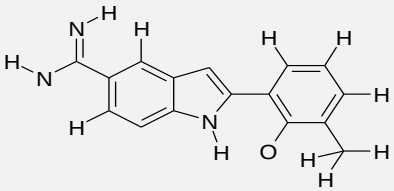	-1.74	-0.36

Processing of molecules:
The set of molecules considered in this study was sketched and geometrically refined using Lig Prep module implemented in the "Maestro suite" program (version 9.5) [20]. After the sketching of all molecules, cleaning and conformational search was performed in "develop pharmacophore" module of PHASE. The conformations were generated by the Monte Carlo (MCMM) method as implemented in Macro Model version 9.5 using a maximum of 1000 steps with a distance-dependent dielectric solvent model and an OPLS-2005 force field. These conformers were employed for the development of pharmacophore model [28, 29].

Pharmacophore mapping:
Phase methodology:
Pharmacophore mapping was carried out using PHASE: a module of Schrödinger's software program 'MAESTRO' [9.5] [34]. This method gives a series of possible common pharmacophore for consideration and hypothesises the imaginary points to be collections of pharmacophoric chemical features i.e (hydrogen-bond donors, hydrogen-bond acceptors, hydrophobic groups, aromatic rings, positive and negative ionic and ionisable centres) contained in the dataset molecules.

Pharmacophore hypothesis generation:
By using "Developing a pharmacophore model" of Phase module, a set of pharmacophore features to create pharmacophore sites (site points) for all the ligands was used. Once a feature has been mapped to a specific location in a conformation, it is referred to as a pharmacophore site. Common pharmacophoric features were then identified from a set of variants-a set of feature types that define a possible pharmacophore. In the next step, common pharmacophore hypothesis were examined using a scoring function i.e. survival scores of actives and inactives [28]. These pharmacophores were scored efficiently using scoring techniques like survival, survival minus inactives and post-hoc, to identify common pharmacophore hypothesis. Each hypothesis was accompanied by a set of aligned conformations that was further used for the alignment of study molecules for 3D- QSAR analysis. PHASE identifies the 3D pharmacophores as 'common feature hypotheses' and ranks them on the basis of how well the alignment of molecules correlates the activities of active and inactive molecules by using vector score , volume score and site score [30]. The regression analysis was performed by constructing a series of models with an increasing number of PLS factors [31].

Docking studies:
The molecular docking tool, Glide (Schrödinger, LLC, New York) software was used for studying binding modes of the compounds in to the binding pocket of caspase. All structures were prepared for docking using 'protein preparation wizard' in Maestro wizard 9.5 [32]. Owing to the increase in computer power and algorithm performance, it is now possible to dock thousands of ligands in a timeline which is useful to the pharmaceutical industry [33].

Compound dataset:
The series of compounds of iodole/ benzoximidazole-5-carboximidine derivatives was docked with the protein urokinase plasminogen activator. The ligands (molecules of dataset) were subjected to Lig Prep wizard work flow, their energies were minimized using OPLS 2005. Ionization of ligand was done between pH 5-9 using Epik ionizer and the stereoisomers were generated at most 32 per ligand. This is an automatic preparation process, performed with the LigPrep tool of the Schrödinger package.

Protein preparation and Receptor grid generation:
Protein structure (PDB ID-1GJ7) was subjected to the Protein Preparation Wizard workflow implemented in the Schrodinger package [29]. The hydrogens were added and water molecules were deleted. Then receptor grid was generated around the binding site. For receptor grid generation, centroid of the workspace ligand was selected by picking and excluding the co-crystallized ligand from the binding site.

Molecular docking:
Molecular docking experiments were carried out by means of the Glide, as implemented in the Schrodinger [34]. A cubing receptor grid was centered around the co-crystallized ligand where the active binding site is present. The XP (extra

precision) scoring function of GLIDE 6.0 was used and lastly the docking job was run.

The scoring function of GLIDE docking program is presented in the G-score form. G-score indicates the binding affinity of the designed compound to the receptor/enzyme.

G Score = 0.05*vd W + 0.15*Coul + Lipo + H bond + Metal + Rewards + Rot B + Site.

where, vdW, Vander Waal energy; Coul, Coulomb energy; Lipo, lipophilic contact term; H Bond, hydrogen-bonding term; Metal, metal-binding term; Bury P, penalty for buried polar groups; RotB, penalty for freezing rotatable bonds; Site, polar interactions at the active site [32].

RESULTS:

Pharmacophore mapping and docking studies were performed on the series of indole/benzoximidazole-5-carboximidine derivatives against uPA to identify common structural features required for the biological activity. These studies were performed with the PHASE module of Schrodinger software.

Pharmacophore mapping:

A total of 5 different variant hypothesis were generated upon completion of common pharmacophore identification process. A maximum of five features were allowed to develop hypothesis. The result of top five hypothesis high gradient score is recorded in **Table 2**.

TABLE 2: SCORING RESULTS OF THE DIFFERENT HYPOTHESES GENERATED

S.no.	ID	Survival	Survival-inactive	Post-hoc	Site	Vector	Volume	Selectivity	# Matches
1	ARRRR.7	3.948	1.572	3.948	1	1	0.949	1.702	4
2	DRRRR.13	3.947	1.798	3.947	1	1	0.949	1.841	4
3	DRRRR.14	3.944	1.621	3.944	1	1	0.947	1.851	4
4	DPRRR.3	3.941	1.557	3.941	0.99	1	0.95	2.353	4
5	APRRR.83	3.941	1.645	3.941	0.99	1	0.947	2.346	4

The top model was found to be associated with the five point hypotheses (APRRR.83) which consist of one acceptor group (A), one positive ionic group (P), three aromatic rings (R). This is denoted as A2P8R9R11R12.The best hypothesis showed the survival score as 3.941. The common pharmacophoric features are then scored with reference to the volume occupied by training set molecules. These large numbers of independent variables are then correlated with dependent variables using Partial Least **S**quares (PLS) analysis [35]. The special disposition of the sites showing distance between pharmacophoric sites is shown in **Fig.1** and the angle between pharmacophoric sites is shown in **Fig.2**.

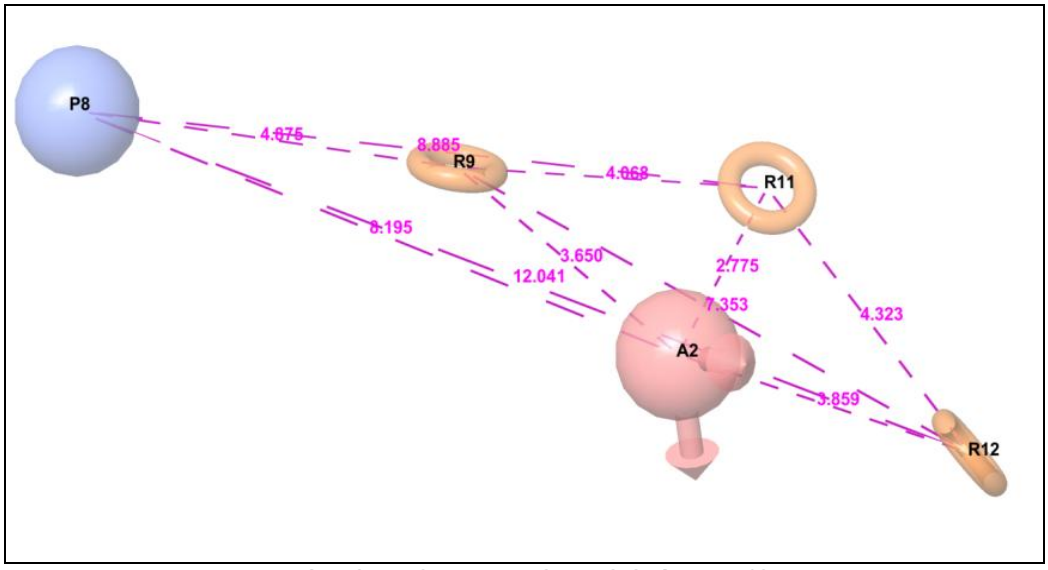

FIG.1: SELECTED HYPOTHESIS: APRRR.83

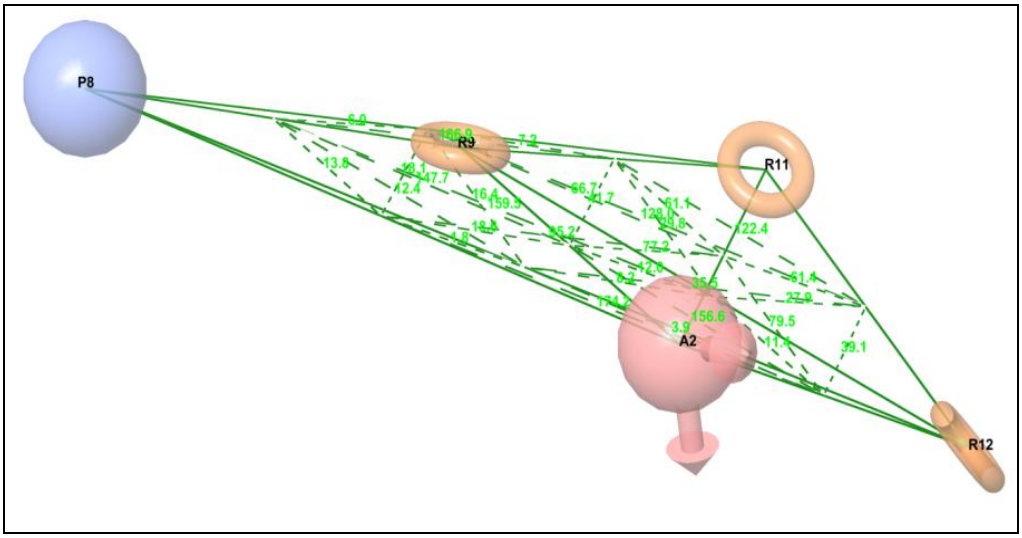

FIG. 2: ANGLES BETWEEN DIFFERENT SITES OF SELECTED HYPOTHESIS: APRRR.83

The pharmacophoric sites mapping over all the molecules of dataset as well as active molecule is shown in **Fig. 3** and **Fig. 4** respectively.

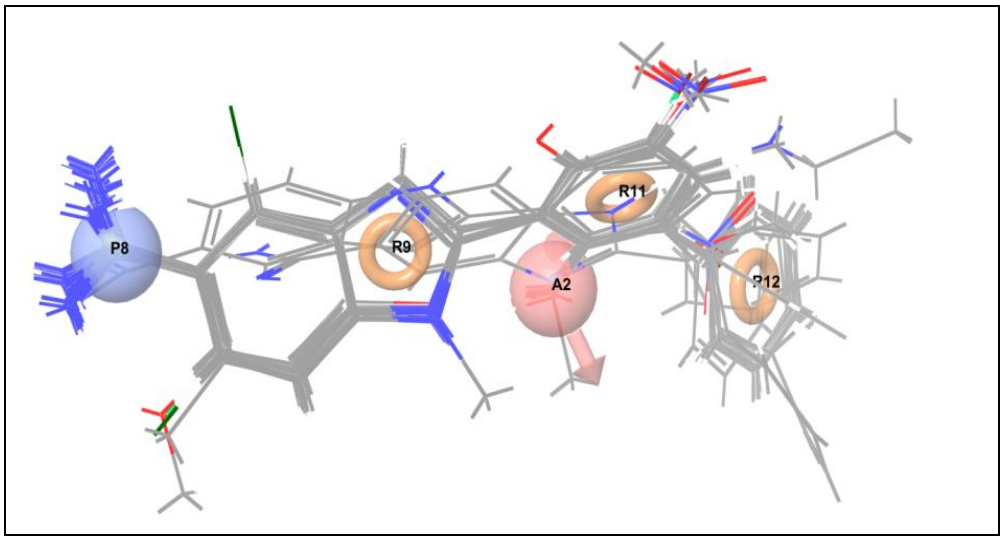

FIG.3: PHARMACOPHORE MAPPED OVER ALL THE MOLECULES OF DATA SET

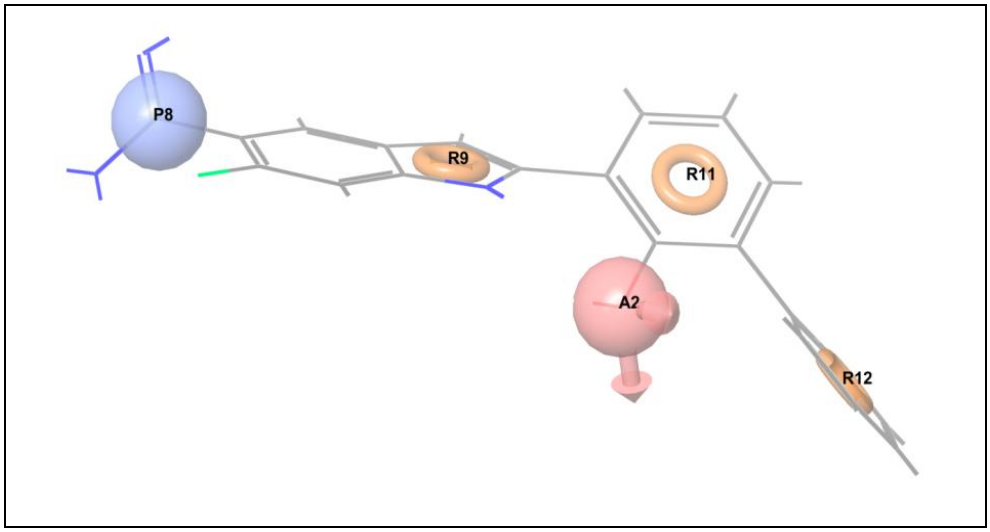

FIG.4: PHARMACOPHORE MAPPED OVER ACTIVE MOLECULE

The pharmacophore hypothesis yielded a 3D-QSAR model with good PLS statistics. Among various PLS factors, PLS factor 5 was selected on the basis of statistical parameters. The training set correlation is characterized by PLS factor 5 (*r*2 = 0.8548, SD = 0.4479, F = 25.9, stability=0.3965). The distances and angles between different sites of ADHHR.515 are given in **Tables 3** and **Table 4** respectively.

TABLE 3: DISTANCES BETWEEN DIFFERENT SITES OF MODEL APRRR.83

Site1	Site2	Distance
A2	P8	8.195
A2	R9	3.65
A2	R11	2.775
A2	R12	3.859
P8	R9	4.875
P8	R11	8.885
P8	R12	12.041
R9	R11	4.068
R9	R12	7.353
R11	R12	4.323

TABLE 4: ANGLES BETWEEN DIFFERENT SITES OF MODEL APRRR.83

Site1	Site2	Site3	Angle
P8	A2	R9	18.6
P8	A2	R11	95.2
P8	A2	R12	174.2
R9	A2	R11	77.2
R9	A2	R12	156.6
R11	A2	R12	79.5
A2	P8	R9	13.8
A2	P8	R11	18.1
A2	P8	R12	1.8
R9	P8	R11	6
R9	P8	R12	12.4
R11	P8	R12	16.4
A2	R9	P8	147.7
A2	R9	R11	41.7
A2	R9	R12	12
P8	R9	R11	166.9
P8	R9	R12	159.5
R11	R9	R12	29.8
A2	R11	P8	66.7
A2	R11	R9	61.1
A2	R11	R12	61.4
P8	R11	R9	7.2
P8	R11	R12	128
R9	R11	R12	122.4
A2	R12	P8	3.9
A2	R12	R9	11.4
A2	R12	R11	39.1
P8	R12	R9	8.2
P8	R12	R11	35.5
R9	R12	R11	27.9

PLS regression analysis, a chemometric technique, was utilized to correlate dependent variables (biological activity) with independent variables (binary values) to derive a 3D-QSAR model [30].It is gaining importance in many fields of chemistry; analytical, physical, clinical chemistry. The pioneering work in PLS was done by H. Wold [36]. PLS creates a series of regression models with PLS factors not larger than 1/5 of the training set molecules. The model was selected on the basis of value of Q^2 and R^2.The generated best model was further validated for its external predictability. For model generation and validation, the total molecules were divided into Training and Test set molecules with training set=28 and test set=11.Differerated models were generated with 5 PLS factors and the best one was selected. The results for the 5 PLS factors are listed in **Table 5**.

TABLE 5: STATISTICAL RESULTS OF GENERATED 3D QSAR MODELS

PLS	SD	R^2	F	Stability	RMSE	Q^2	Pearson-R
1	0.7757	0.4853	24.5	0.8383	0.6769	0.1981	0.4721
2	0.6709	0.6298	21.3	0.6964	0.6218	0.3231	0.6566
3	0.5809	0.7336	22	0.6516	0.5842	0.4026	0.7507
4	0.5081	0.8047	23.7	0.4675	0.5302	0.5079	0.797
5	0.4479	0.8548	25.9	0.3965	0.4938	0.5732	0.8244

The model generated with PLS 5 was selected as the best model with correlation coefficient R^2=O.8548. The reliability of the model can be judged based on the external prediction. The model showed very good correlation coefficient of 0.8244 with the test set molecules. The predicted activity of training and test set molecules are presented in the **Table 1** and the fitness scores are shown of all the molecules of dataset is shown in **Table 6**.

TABLE 6: FITNESS SCORES OF ALL THE TRAINING AND TEST SET COMPOUNDS.

Ligand Name	Pharm Set	QSAR Set	Fitness
s1		training	2.27
s2		training	2.25
s3		training	2.26
s4		Test	2.26
s5		training	2.23
s6		Test	2.37
s7		training	2.3
s8		training	2.31
s9		Test	2.33
s10		Test	2.78
s11		training	2.25
s12		training	2.22
s13		training	2.28
s14		training	2.32
s15		Test	2.32
s16		Test	2.36
s17		training	2.38
s18		Test	2.29
s19		training	2.96
s20	active	training	2.88
s21	inactive	training	2.21
s22		training	2.64
s23	inactive	training	2.72
s24		training	2.92
s25	active	training	**3**
s26		training	2.98
s27	active	training	2.98
s28	active	training	2.99
s29		training	2.99
s30		Test	2.96
s31		Test	2.22

s32	inactive	training	2.21
s33		training	2.78
s34		training	2.36
s35		Test	2.94
s36		training	2.94
s37		Test	2.88
s38		training	1.38
s39	inactive	training	2.37

The correlation scatter plot between actual and predicted values of biological activity of training and test set is presented in **Fig.5**.

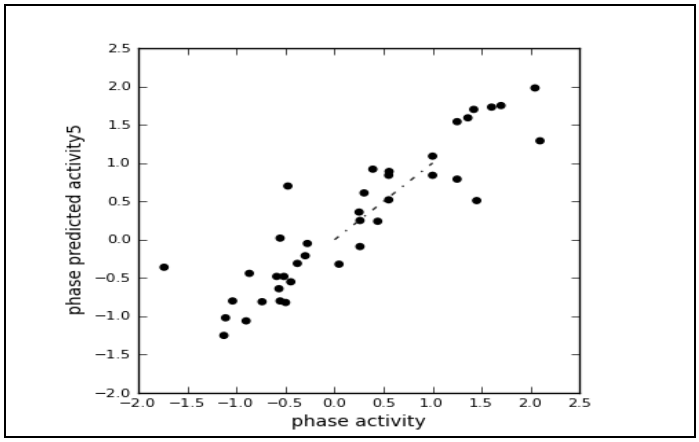

FIG. 5: CORRELATION SCATTER PLOT ACTUAL AND PREDICTED ACTIVITY OF TRAINING AND TEST SET MOLECULES.

Contour analysis:

Contour plots generated from the best 3D QSAR model are represented as positive and negative activity coefficient of different properties, namely hydrogen bond donor (A), hydrophobic/non-polar (B) and electron withdrawing (C) properties are given in **Fig. 6**. The blue contours represent the regions where the substitution of groups with the particular property may enhance the biological activity whereas red cubes represent the depreciating biological activity.

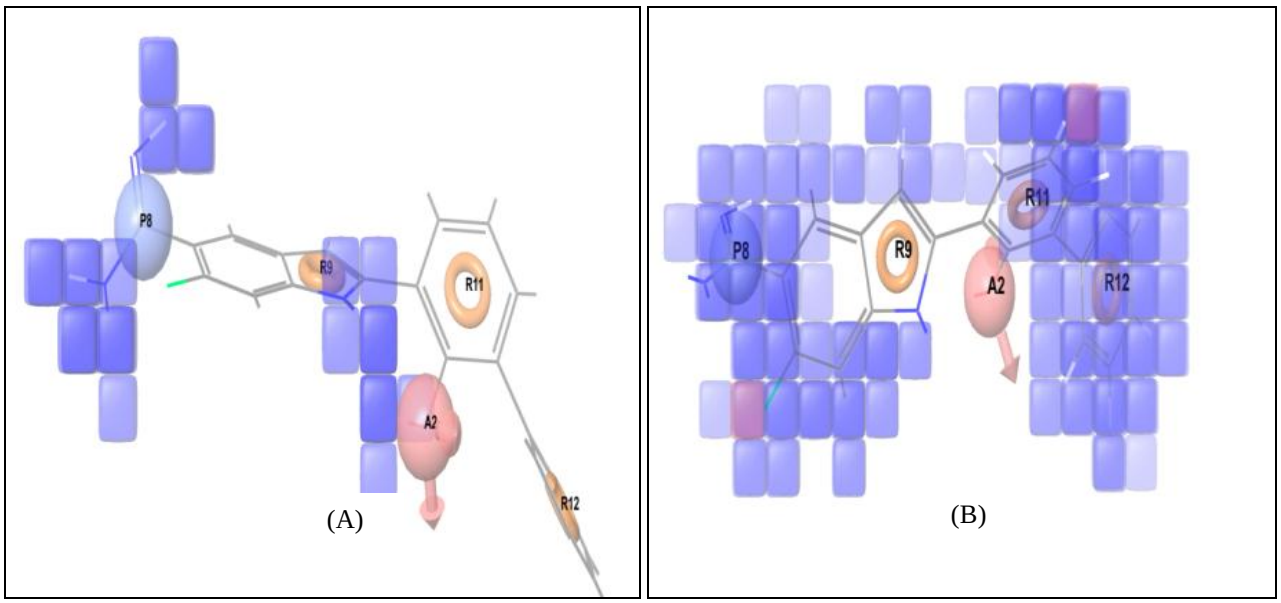

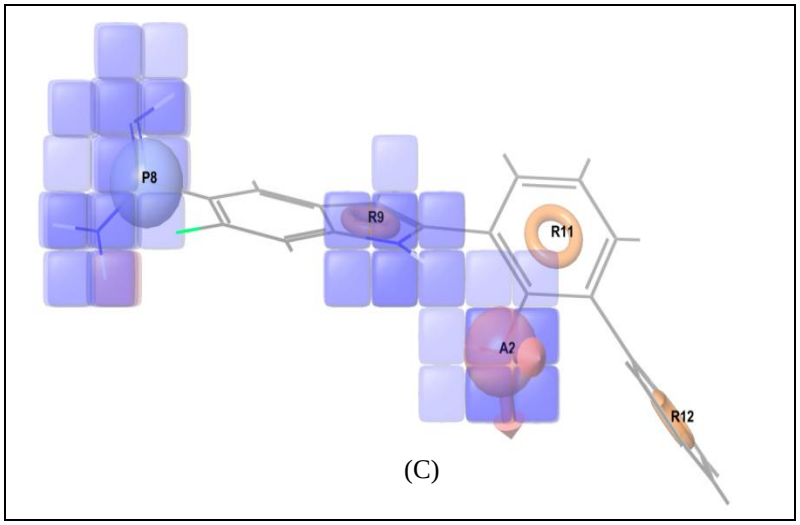

FIG. 6: STRUCTUREOVIEWS OF CONTOUR MAPS FOR 3D-QSAR MODELS HYDROGEN BOND DONOR (A), HYDROPHOBIC (B) AND ELECTRON WITHDRAWING PROPERTY (C).

A) Hydrogen bond donor property contour:

As shown in the **Fig. 6A**, a large blue contour at 5th position of indole moiety signifies the importance of H-bond donor group at this position. This H-bond donor group (carboximidine) is important for the anti-cancer activity of all the compounds of dataset. The blue region at Nitrogen of Indole and Hydroxyl group of biphenyl ring indicates the importance of indole ring and hydroxyl group for the activity. Compounds s16,s 17, s18, s19, s20, s25, s26, s27, s28, s34, s35, s36, s37with indole ring and hydroxyl group of biphenyl ring showed comparative activity as s25.

B) Hydrophobic property contour:

Contour map for hydrophobic property displayed in **Fig. (6B)** displays the most active compound as orienting itself into the favourable blue region. The blue region at position 1,3,4,5,6,7 and around biphenyl are in favourable region of positive activity coefficient thereby increasing the activity whereas in other most compounds less hydrophobic hydrogen group at position 6th is present in favourable region thereby reducing the activity compared to s25.

C) Electron withdrawing property contour:

A large blue contour at 5th position of indole moiety **Fig. (6C)** signifies the importance of electron withdrawing group at this position. This electron withdrawing group (carboximidine) is important for the anti-cancer activity of all the compounds of dataset. The blue region at 1st and 2nd position of Indole and Hydroxyl group of biphenyl ring indicates the importance of these region for the activity.

Docking studies:

The docking studies were carried out to explore the interaction mechanism between inhibitors and the receptor. The final evaluation is done with glide score (docking score) and best pose is generated as the output.

G score = a x vdw + b* cow þ Lipo +H bond+ Metal + BuryP + Rot B + Site

where, vdW, Vander Waal energy; Coul, Coulomb energy; Lipo, lipophilic contact term; H Bond, hydrogen-bonding term; Metal, metal-binding term; Bury P, penalty for buried polar groups; RotB, penalty for freezing rotatable bonds; Site, polar interactions at the active site [26]. The 3D view of uPA is shown in **Fig.7**.

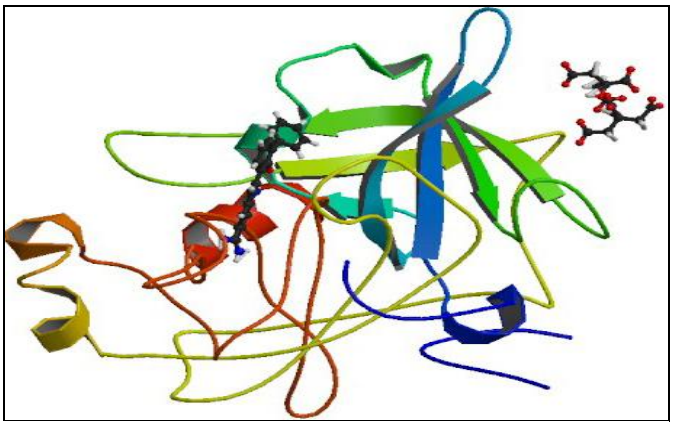

FIG. 7: 3D VIEW OF UROKINASE-TYPE PLASMINOGEN ACTIVATOR (PDB ID-1GJ7

The most active compound in the training set has scored a best docking score value of -11.89. It has formed an interaction with HIS57, ASP219, GLY189, SER 190. The Glide scores and other solutions of protein-ligand complexes obtained from docking calculations for selected compound are listed in **Table 7**.

TABLE 7: DOCKING SCORES AND OTHER SOLUTIONS OBTAINED FOR THE MOST ACTIVE LIGAND

Ligand	S25
Gscore	-11.89
Lipophilic Evd W	-6.18
Phob En	0
PhobEnHB	0
PhobEnPairHB	0
Hbond	-2.56
Electro	-2.56
Sitemap	-0.38
PiCat	0
ClBr	0
LowMW	-0.35
Penalties	0
HBPenal	0
ExposPenal	0.12
RotPenal	0.1

The ligand protein interaction in 2D view is shown in **Fig.8** and **Fig. 9** shows the 3D view of docking of most active ligand into binding pockets of uPA.

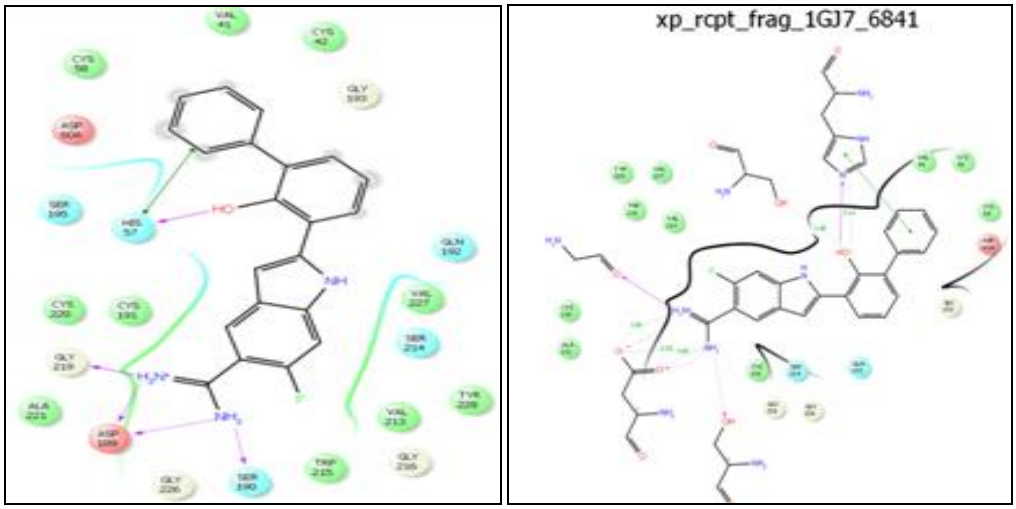

FIG. 8: DOCKING INTERACTION POSE OF MOST ACTIVE LIGAND (25) WITH UROKINASE TYPE PLASMINOGEN ACTIVATOR.

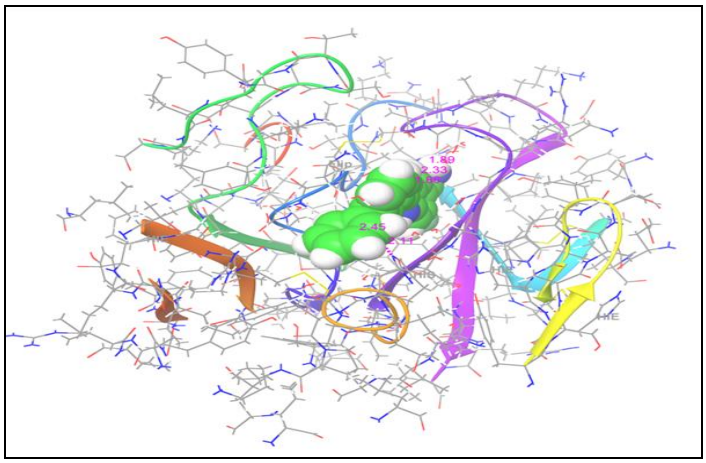

FIG.9: THE BINDING POCKET OF uPA (PDB ID: 1GJ7) WITH THE MOST ACTIVE COMPOUND S25.

To validate the docking protocol, co-crystallized ligand (132) was docked into the active site of urokinase plasminogen activator (1GJ7). The Glide scores and other solutions of protein-ligand complexes obtained from docking calculations for selected compound are listed in **Table 8**.

TABLE 8: DOCKING SCORES AND OTHER SOLUTIONS OBTAINED FOR THE CO-CRYSTALLIZED LIGAND

Ligand	Reference
GScore	-11.626
LipophilicEvdW	-6.4943
PhobEn	0
PhobEnHB	0
PhobEnPairHB	0
HBond	-2.411548
Electro	-2.635966
Sitemap	0
PiCat	0
ClBr	0
LowMW	-0.29056
Penalties	0
HBPenal	0
ExposPenal	0.118857
RotPenal	0.087536

The co-crystallized ligand protein interaction in 2D view is shown in **Fig.10** and **Fig.11** shows the 3D view of docking of co-crystallized ligand into binding pockets of uPA (urokinase-type plasminogen activator).

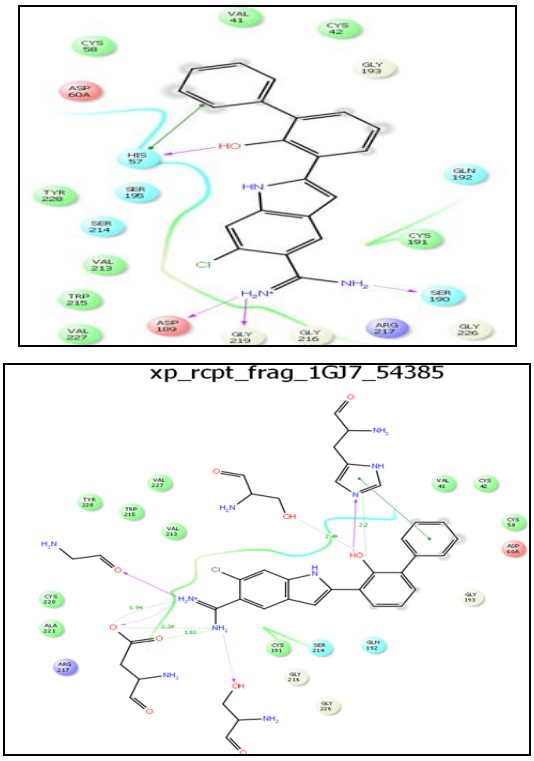

FIG 10: DOCKING INTERACTION POSE OF CO-CRYSTALLIZED LIGAND WITH UROKINASE TYPE PLASMINOGEN ACTIVATOR

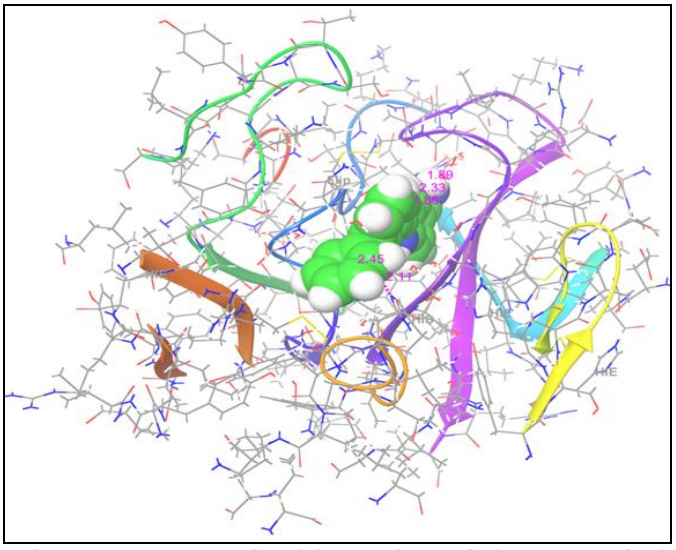

FIG.11: THE BINDING POCKET OF uPA (PDB ID: 1GJ7) WITH THE CO-CRYSTALLIZED LIGAND OF THE PROTEIN

Interactions in Docking:

A) Ligand s25:

The hydroxyl group (OH) of phenyl showed the H-bond interaction (distance=2.11Å) with the nitrogen atom of imidazole ring of HIS57 amino acid of the protein residue. The positively charged NH2 group of the indole ring showed a H-bond interaction (distance=1.91659Å) with the oxygen of carbonyl group of GLY219 and a H-bond interaction (distance=1.89 Å) with the oxygen of hydroxyl group of ASP 189 3amino acids and the other NH2 showed a H-bond interaction (distance=1.86 Å) with the oxygen of carbonyl group ASP 189 and H-bond interaction (distance=2.00 Å) with the oxygen of hydroxyl group of SER190 amino acids of the protein. Also the terminal phenyl group of ligand showed a pi-pi stacking (distance=4.81689Å) with the imidazole ring of HIS57.

B) Co-crystallized Ligand:

The hydroxyl group (OH) of phenyl showed the H-bond interaction (distance=2.2Å) with the nitrogen atom of imidazole ring of HIS57 amino acid of the protein residue. The positively charged NH2 group of the indole ring showed a H-bond interaction (distance=1.90873Å) with the oxygen of carbonyl group of the GLY219 and H-bond interaction (distance=1.94Å) with the oxygen of hydroxyl group of ASP 189 amino acids and the other NH2 showed a H-bond interaction (distance=2.02609Å) with the oxygen of hydroxyl group of SER190

amino acid of the protein. Also the terminal phenyl group of ligand showed a pi-pi stacking (distance=4.84263 Å) with the imidazole ring of HIS57.

DISCUSSION: In the present studies, PHASE and GLIDE modules were employed to a series of indole/ benzoimidazole-5-carboxamidines as uPA inhibitors. PHASE identifies the 3D pharmacophores as 'common feature hypotheses' and ranks them on the basis of how well the alignment of molecules correlates the activities of active and inactive molecules by using vector score, volume score and site score. The regression analysis was performed by constructing a series of models with an increasing number of PLS factors. PLS creates a series of regression models with PLS factors not larger than 1/5 of the training set molecules. The pharmacophore hypothesis yielded a 3D-QSAR model with good PLS statistics. The model was selected on the basis of value regression coefficient and co-relation coefficient.

Contour plots generated from the best 3D QSAR model are represented as positive and negative activity coefficient of different properties, namely hydrogen bond donor (A), hydrophobic/non-polar (B) and electron withdrawing (C) properties The blue contours represent the regions where the substitution of groups with the particular property may enhance the biological activity whereas red cubes represent the depreciating biological activity. The series of compounds of iodole/ benzoximidazole-5-carboximidine derivatives was then docked with the protein urokinase plasminogen activator. The ligands (molecules of dataset) were subjected to LigPrep wizard work flow, their energies were minimized using OPLS 2005. Ionization of ligand was done and the stereoisomers were generated at most 32 per ligand.

This is an automatic preparation process, performed with the LigPrep tool of the Schrödinger package. The XP (extra precision) scoring function of GLIDE 6.0 was used. The scoring function of GLIDE docking program is presented in the G-score form. G-score indicates the binding affinity of the designed compound to the receptor/enzyme. The docking studies were carried out to explore the interaction mechanism between inhibitors and the receptor. To validate the docking protocol, co-crystallized ligand (132) was docked into the active site of urokinase plasminogen activator (1GJ7).

CONCLUSION: Pharmacophore mapping studies were performed on indole/benzoimidazole-5-carboxamidine derivatives to determine the structural requirements for potency against uPA (urokinase-type plasminogen activator) for their anticancer activity. A highly predictive pharmacophore based 3D-QSAR model was generated with five point hypotheses (APRRR) with one acceptor atom, one positively charged group and three aromatic rings as pharmacophore features.

To explore the lead optimization options of the Indole / benzoimidazole – 5 - carboxamidine derivatives, this dataset was used to build a QSAR model where the model with best statistics found was with PLS factor 5 with best correlation coefficient (R2=0.8548), standard deviation (0.4479) and variance ratio (F) (25.9). This model showed correlation coefficient (Q2) 0.5732 and Pearson R (0.8244**)** with test set molecules. Contour analysis from our model gave us the following vital information about our core molecule. Hydrogen bond donor and electron withdrawing group at 5^{th} position of indole ring (carboximidine) is important for the activity. Indole ring itself plays a significant role in anticancer activity. Biphenyl substituent at 2^{nd} position of indole ring is in favourable region of positive activity coefficient.

Electron withdrawing group (hydroxyl) at 2' position of biphenyl ring leads to increase in activity as in compound s25. More hydrophobic group than hydrogen at 6^{th} position of indole ring as fluorine, chlorine leads to increase in activity. The binding interactions of the database uPA inhibitors in the active site were studied by molecular docking. The scoring function of GLIDE docking program is presented in the G-score form which indicates the binding affinity of the designed compound to the receptor/enzyme. The Gscore of the ligand no. s25 was found to be -11.89 as comparable with the G-score of reference drug i.e. -11.626. The present study aimed to develop ligand based pharmacophore hypothesis and a

interaction pattern by docking. Both studies rendered significant information which gives detailed structural insights as well as highlights important binding features of uPA inhibitors which can provide crucial clues and guidance that can be used in the successful designing of novel highly active analogues against uPA.

ACKNOWLEDGEMENT: One of the author wish to acknowledge to the AICTE (All India Council of Technical Education) for granting of the fund for the completion of this project work.

REFERENCES:

1. Jurado RB, González TA, Chávez BL, Peña A, Navarro RC, Hernan A: Circulating Levels of Urokinase-Type Plasminogen Activator Receptor and D-Dimer in Patients With Hematological Malignancies. Clinical Lymphoma Myeloma and Leukemia. 2015; 15:621–626.
2. Enocsson H, Wetterö J, Skogh T, Sjöwall C: Soluble urokinase plasminogen activator receptor levels reflect organ damage in systemic lupus erythematosus. Translational Research. 2013; 162:287–296.
3. Paland N, Lazarovich GA, Coleman R, Fuhrman B: Urokinase-type plasminogen activator (uPA) stimulates triglyceride synthesis in Huh7 hepatoma cells via p38-dependent upregulation of DGAT2. Atherosclerosis. 2014; 237:200–207.
4. Salvatore U, Enke B, Salvatore S, Massimino A: The Urokinase Plasminogen Activator System: A Target for Anti-Cancer Therapy. Current Cancer Drug Targets. 2009; 9:32- 71.
5. Llinas P, Le Du MH, Gårdsvoll H: Crystal structure of the human urokinase plasminogen activator receptor bound to an antagonist peptide. Journal of Europeon Molecular Biology Organisation 2005; 24:1655–63.
6. Huai Q, Mazar AP, Kuo. A: Structure of human urokinase plasminogen activator in complex with its receptor. Science. 2006; 311:656–9.
7. Choong PF, Nadesapillai AP. Urokinase plasminogen activator system: a multifunctional role in tumor progression and metastasis. Clinical Orthopaedics and Related Research. 2003; 415:S46-58.
8. Anand P.K, Kunnumakara AB, Sundaram C, Harikumar KB, Tharakan ST, Lai OS, Sung B, Aggarwal BB: Cancer is a preventable disease that requires major lifestyle changes. Pharmaceutical Research. 2008; 25:2097–116.
9. Kenneth K, Vogelstein B.W: Introduction- The genetic basis of human cancer, 2nd ed. McGraw-Hill. New York. 2002.
10. American Cancer Society. Heredity and Cancer. http://www.cancer.org/cancer/ cancercauses/ genetics and cancer/heredity-and-cancer. 2013.
11. Zali H, Tavirani M.R, Mona A: Gastric cancer: prevention, risk factors and treatment. Gastroenterology and Hepatology From Bed to Bench. 2011; 4:175-85.
12. American Cancer Society. Cancer Prevention & Early Detection Facts & Figures. http://www.cancer.org/ acs/groups/content/@epidemiologysurveilance/documents/ document/acspc-037535.pdf. 2013.
13. Copper G.M: Elements of human cancer. Jones and barlett publishers.
14. Larsson S.C, Wolk. A: Coffee consumption and risk of liver cancer: a meta-analysis. Gastroenterology. 2007; 132:1740-1745.
15. Bhongade B.A, Gadad A.K: 3D-QSAR CoMFA/CoMSIA studies on Urokinase plasminogen activator (uPA) inhibitors: a strategic design in novel anticancer agents. Bioorganic & Medicinal Chemistry. 2004; 12:2797–2805.
16. Sethi S, Navdeep: A review on computational methods in developing quantitative structure-activity relationship (QSAR). International journal of drug research and technology. 2012; 2:313-41.
17. Cronin, M.T.D, Leszczynski J: In: Quantitative structure–activity relationships (QSARS) – applications and methodology. Spinger. 2010; 8:3-11.
18. Yang, Sheng Y: Pharmacophore Modelling and applications in drug discovery: challenges and recent Advances. Drug Discovery today. 2010; 15:444-50.
19. Sakkiah S, Krishnamoorthy N, Gajendrarao P, Thangapandian S, Lee Y, Kim S, Suh JK, Kim HH, Lee WK: Pharmacophore Mapping and Virtual Screening for SIRT1 Activators. Bulletin of the Korean Chemical Society. 2009; 30:1-5.
20. Phase, version 3.6, Schrödinger, LLC, New York, NY, 2013.
21. Lengauer T, Rarey M: Computational methods for biomolecular docking. Current Opinion of Structural Biology. 1996; 6:402-6.
22. Kitchen B.D, Decornez H, Furr RJ, Bajorath J: Docking and scoring in virtual screening for drug discovery: methods and applications. Nature reviews Drug discovery. 2004; 3:935–49.
23. Vijayakumar B, Dheen PK, Vijayakumar B: Molecular docking studies – a review. International Journal of Medicinal Chemistry & Analysis. 2012; 2:106-111.
24. Srivastav B, Batra N, Sahu S, Solanki R, Lokwani P: Molecular Modeling: Necessary tool for drug designing. International Journal of Pharmaceutical Erudition. 2011; 1:81-92.
25. Martin CY: Applications of Pharmacophore Mapping. Reference Module in Chemistry, Molecular Sciences and Chemical Engineering. 2014.
26. Fidom K, Isberg V, Hauser SA, Mordalski S, Lehto T, Bojarski JA, Gloriam ED: A new crystal structure fragment-based pharmacophore method for G protein-coupled receptors. Methods. 2015; 71: 104–112.
27. Bjerrum JE: Machine learning optimization of cross docking accuracy. Computational Biology and Chemistry. 2016; 62:133–144.
28. Mehta H, Lal K, Sukhbir A, Kanika K, Pawan: Pharmacophore mapping and 3D-QSAR analysis of *Staphylococcus aureus* Sortase inhibitors. Journal for Medicinal Chemistry, Pharmaceutical Chemistry and Computational Chemistry. June 2012; 4:1776-84.
29. Maestro, version 9.5, Schrödinger, LLC, New York, NY, 2013.
30. Vazhapullya MA, Vinod BD, Zeinul HNH: Pharmacophore and 3D QSAR Study of TGFβ Inhibitors. Letters in Drug Design & Discovery. 2014; 11: 1570-808.
31. Kaur P, Sharma V, Kumar V: Pharmacophore Modelling and 3D-QSAR Studies on N3 -Phenylpyrazinones as Corticotropin-Releasing Factor 1Receptor Antagonist. International Journal of Medicinal Chemistry. 2012; doi:10.1155/2012/452325.
32. Asgaonkar DK, Mote DG, Chitre TS: QSAR and Molecular docking studies of oxadiazole ligated Pyrrole

derivatives as Enoyl ACP co Reductase Inhibitors. Scientia pharmaceutica. 2014; 82:71-85.
33. Taylor RD, Jewsbury PJ, Essex JW: A review of protein-small molecule docking methods. Journal of Computer-Aided Molecular Design. 2002; 16:151–66.
34. Glide, Version 6.0, Schrodinger, LLC, New York, NY, 2013.
35. Dixon SL, Smondyrev AM, Knoll EH, Rao SN, Shaw DE, Friesner RA: "PHASE: A New Engine for Pharmacophore Perception, 3D QSAR Model Development, and 3D Database Screening. 1. Methodology and Preliminary Results". J of Computer-Aid Mol Design 2006; 20:647-71.
36. Geladi P, Kowalski B: Partial least Square-A tutorial. Analytica Chimica Acta. 1986; 185:1–17.

How to cite this article:
Agarwal S, Mishra M, Mishra VK, Vinod D, Verma E and Kashaw SK: *In-silico* Pharmacophore Mapping and Docking Studies of Indole/Benzoximidazole-5-Carboximidine Derivatives as Anti-Cancer Agents. Int J Pharm Sci Res 2016; 7(8): 3243-61.doi: 10.13040/IJPSR.0975-8232.7(8).3243-61.